

# A second-generation assembly of the *Drosophila simulans* genome provides new insights into patterns of lineage-specific divergence

Tina T. Hu,<sup>1,4</sup> Michael B. Eisen,<sup>2</sup> Kevin R. Thornton,<sup>3</sup> and Peter Andolfatto<sup>1</sup>

<sup>1</sup>Department of Ecology and Evolutionary Biology and the Lewis-Sigler Institute for Integrative Genomics, Princeton University, Princeton, New Jersey 08544, USA; <sup>2</sup>Howard Hughes Medical Institute and the Lawrence Berkeley Laboratory, University of California Berkeley, Berkeley, California 94720, USA; <sup>3</sup>Department of Ecology and Evolutionary Biology, University of California Irvine, Irvine, California 92617, USA

We create a new assembly of the *Drosophila simulans* genome using 142 million paired short-read sequences and previously published data for strain *w*<sup>501</sup>. Our assembly represents a higher-quality genomic sequence with greater coverage, fewer misassemblies, and, by several indexes, fewer sequence errors. Evolutionary analysis of this genome reference sequence reveals interesting patterns of lineage-specific divergence that are different from those previously reported. Specifically, we find that *Drosophila melanogaster* evolves faster than *D. simulans* at all annotated classes of sites, including putatively neutrally evolving sites found in minimal introns. While this may be partly explained by a higher mutation rate in *D. melanogaster*, we also find significant heterogeneity in rates of evolution across classes of sites, consistent with historical differences in the effective population size for the two species. Also contrary to previous findings, we find that the X chromosome is evolving significantly faster than autosomes for nonsynonymous and most noncoding DNA sites and significantly slower for synonymous sites. The absence of a X/A difference for putatively neutral sites and the robustness of the pattern to Gene Ontology and sex-biased expression suggest that partly recessive beneficial mutations may comprise a substantial fraction of noncoding DNA divergence observed between species. Our results have more general implications for the interpretation of evolutionary analyses of genomes of different quality.

[Supplemental material is available for this article.]

The completion of genomes for an increasing number of eukaryotic species promises unprecedented power to distinguish among models of genome evolution. Population genetic theory predicts that the amount of divergence along a species lineage should depend on the mutation rate, the strength and mode of natural selection, and the species effective population size ( $N_e$ ), as well as the genomic context such as sex linkage, recombination rate, and other factors (Kimura 1983; Charlesworth et al. 1987, 2009). How these factors ultimately contribute to observed patterns of genome evolution is an empirical question that has been the subject of intense investigation in population genetics for the past several decades (Charlesworth 2010).

Studies of *Drosophila*, particularly *Drosophila melanogaster* and its close relatives, have historically been at the forefront of such investigations. Ohta (1993) first raised the point that the protein alcohol dehydrogenase evolves more quickly in Hawaiian *Drosophila* than other Drosophilids, consistent with a reduction in the efficacy of purifying selection on weakly deleterious amino acid substitutions associated with smaller  $N_e$  in this species. Ohta also noted elevated rates of protein evolution in primates and rodents, again, consistent with smaller  $N_e$  in these species than in many Drosophilids. Using a larger collection of genes, Akashi (1995, 1996) showed that rates of synonymous and nonsynonymous substitution are higher in the *D. melanogaster* lineage relative to the

*Drosophila simulans* lineage, consistent with a historically smaller  $N_e$  and concomitantly relaxed selection on slightly deleterious mutations at these sites in *D. melanogaster* (Aquadro et al. 1988; Moriyama and Powell 1996).

Since these seminal studies, numerous follow-up studies on *Drosophila* and other species have tested the relationship between population size, genomic context (i.e., recombination rate and sex linkage), and lineage-specific rates of evolution. Broadly speaking, these studies have found patterns that are consistent with the nearly neutral evolution view with respect to lineage-specific rates of evolution and effects of chromosomal context (Wright and Andolfatto 2008; Charlesworth et al. 2009; Mank et al. 2010). However, there are exceptions, and recent studies based on genome-wide analyses suggest a more complex picture. For example, in the first genome-wide comparison of the *D. melanogaster* and *D. simulans* lineages, Begun et al. (2007) found significantly greater levels of divergence for nonsynonymous, synonymous and 5' untranslated region (UTR) sites in the *D. melanogaster* lineage, but the opposite pattern for introns, intergenic, and 3'-UTR regions. This finding is unexpected given the "smaller  $N_e$  in *D. melanogaster*" interpretation for the differential accumulation of synonymous and nonsynonymous substitutions in the two lineages. Since introns, intergenic, and 3'-UTR regions, like 5' UTRs, nonsynonymous, and synonymous sites are all subject to purifying selection in both *D. melanogaster* and *D. simulans* (Andolfatto 2005; Haddrill et al. 2008), we expect asymmetric levels of divergence in the two lineages in the same direction, albeit to different extents.

Likewise, previous analyses comparing rates of evolution on the X versus the autosomes have also revealed complex patterns. If

#### <sup>4</sup>Corresponding author E-mail [tthu@princeton.edu](mailto:tthu@princeton.edu)

Article published online before print. Article, supplemental material, and publication date are at <http://www.genome.org/cgi/doi/10.1101/gr.141689.112>. Freely available online through the *Genome Research* Open Access option.

most of genome evolution is due to the accumulation of neutral and slightly deleterious variants that are at least partially recessive, we expect that the X chromosome will evolve more slowly than the autosomes, while the opposite pattern is expected if a large fraction of genome evolution is due to partly recessive beneficial substitutions (Charlesworth et al. 1987). In this context, Begun et al. (2007) found some evidence that the X evolves faster than autosomes in the two species; however, the detailed pattern was complex. For example, the pattern appears to be inconsistent in the two species lineages, with X-linked intronic and intergenic regions evolving significantly slower than autosomes in *D. melanogaster*, but at the same rate or significantly faster in *D. simulans* (see Table S3 of Begun et al. 2007).

One is left wondering about the cause of these complex patterns of divergence among different annotations of sites and chromosomal contexts. In one sense, they are perhaps not surprising given the plurality of population genetic processes, with models of negative and positive selection predicting effects in opposing directions. Other factors, such as differences in mutation rate, may also play a role. For example, Begun et al. (2007) cite hypertranscription of genes on the X, associated with dosage compensation, as possibly elevating mutation rates on the X chromosome (although this seems at odds with their finding of a significantly slower X for introns in *D. melanogaster*).

Differences in patterns of divergence in the *D. melanogaster* and *D. simulans* lineages suggest potentially interesting differences in biology between the species. However, a possible concern in overinterpreting such analyses is the quality of the *D. simulans* genome reference sequence relative to that of *D. melanogaster*. In particular, the *D. simulans* assembly represents a composite of six independently derived strains, each with only partial coverage of the genome (Begun et al. 2007). Even when combined, the *D. simulans* genome has the lowest Q20 coverage (number of assembled reads with an average quality score of 20) of the initial 12 sequenced *Drosophila* genomes (*Drosophila* 12 Genomes Consortium et al. 2007). The *D. simulans* reference genome is also represented in 10,005 scaffolds, with the assembly of the six major chromosome arms (X, 2L, 2R, 3L, 3R, and 4) containing just 101.3 Mb of the expected 137.8 Mb (based on the *D. melanogaster* reference genome). In addition, genomic DNA from a mixture of males and females was sequenced, implying that the X chromosome has lower coverage on average than the autosomes (since there will be three copies of the X chromosome for every four copies of the autosomes). The difference in coverage between the X and autosomes makes a quantitative comparison of rates of evolution on these chromosomes difficult. Finally, a recent linkage analysis based validation of the *D. simulans* genome revealed several major misassemblies in the *D. simulans* genome (Andolfatto et al. 2011a).

To address concerns regarding quality and completeness of the *D. simulans* genome, we have created a new assembly by combining high-coverage Illumina short-read sequence data with previously published Sanger sequence data from a single strain. By sequencing females, we effectively balance sequence coverage between the X and autosomes. Using this improved sequence, we revisit analyses of genome-wide divergence along the *D. melanogaster* and *D. simulans* lineages and document some surprising differences with previous analyses. In particular, we find consistently higher rates of divergence along the *D. melanogaster* lineage for all types of sites, including the putatively neutral “fastest-evolving sites” of short introns, implying that all such sites are under weak purifying selection or a higher mutation rate in the *D. melanogaster* lineage. In addition, in both *D. melanogaster*

and *D. simulans*, we find faster-X divergence at nonsynonymous, introns longer than 100 bp, and UTR sites, but not other sites, consistent with recessivity of positively selected mutations or a different composition of genes on the X chromosome and autosomes. We discuss the implications of our findings in the context of ongoing low-coverage genome sequencing projects and how coverage and quality ultimately affect the reliability of evolutionary inferences in comparative genomic studies.

## Results

### Sequencing and assembly

We created a de novo assembly of the *D. simulans* genome by combining new sequence data (142 million 104-bp and 101-bp paired-end Illumina reads) with previously published Sanger sequence data for strain *w<sup>501</sup>* (Supplemental Table 1) using the Velvet assembler (Zerbino and Birney 2008). Our de novo assembly comprises 21,613 contigs totaling 124.2 Mb with an  $N_{50}$  of 150 kb (Supplemental Table 2), a considerable improvement over the previous assembly's  $N_{50}$  of 17 kb (*Drosophila* 12 Genomes Consortium et al. 2007). It is generally expected that repetitive DNA should limit the efficiency of de novo assembly (Treangen and Salzberg 2012). We find that our 500-bp insert libraries, combined with the published 3-kb insert paired-end Sanger data, is sufficient to assemble contigs despite the presence of (albeit small) internal repetitive elements (Supplemental Figs. 1, 2). An estimated 6.85% of our assembly corresponds to annotated transposons in *D. melanogaster* (see Methods), where most of the contigs containing transposable elements are dominated by contigs smaller than 500 bp (Supplemental Fig. 1B). This said, a repetitive element was found within 500 bp of the end in only 7% of contigs >3 kb, and of this set, 58% had an element at both ends. Thus, transposable elements do not appear to be a major factor limiting our assembly of larger contigs.

We assembled Velvet contigs into scaffolds using the *D. melanogaster* reference sequence as a guide (see Methods). A schematic of this approach is shown in Supplemental Figure 3. A total of 2156 contigs map uniquely to the *D. melanogaster* reference genome and the final assembly of chromosomes X, 2, 3, 4, and the mtDNA genome totals 118.5 Mb (Table 1). This represents 95.4% of the expected genome size based on the sum of contig lengths generated by the Velvet assembly. Read depth across the entire assembly centers around 75× with comparable sequence coverage between the X and autosomes (Supplemental Fig. 4; Supplemental Table 3). An additional 19,596 contigs (totaling 8.3 Mb) remain unassembled and correspond primarily to repetitive regions and/or unassembled regions of the *D. melanogaster* reference assembly. We fail to uniquely map Velvet contigs to 3.15% (3,580,129 bp) of

**Table 1.** Assembled chromosome size (non-N base pairs)

Chromosome	Dsim <sub>ref</sub>	Dsim <sub>w501</sub>	Increase (bp)	% increase
X	14,430,506	20,841,377	6,410,871	44.43
2L	20,694,621	23,580,698	2,886,077	13.95
2R	18,189,903	21,589,632	3,399,729	18.70
3L	21,194,319	24,255,573	3,061,254	14.44
3R	25,966,479	27,161,151	1,194,672	4.60
4	807,946	1,026,555	218,609	27.06
Subtotal	101,283,774	118,454,986	17,171,212	16.95
mtDNA	—	17,860	—	—
Unassembled	28,132,509	8,300,655	—	—

a “TE-minimized” version of the *D. melanogaster* reference genome (see Methods). These regions in the *D. melanogaster* reference genome generally corresponded to repetitive or low complexity regions where determining the uniqueness of mapped Velvet contigs was difficult.

Of the 13,717 annotated genes in *D. melanogaster*, orthologs were determined for 13,281 genes (96.8%) in our *D. simulans* assembly. Relative to *D. melanogaster*, we detected 35 transposition events between chromosome arms (ICT) and 374 putative local rearrangement (LR) events in our assembly (Supplemental Table 4). When incorporating *Drosophila yakuba*, the number of orthologs found in all three species reduces to 12,747 genes (92.9% of *D. melanogaster* genes). From this subset, rates of evolution along the *D. melanogaster* and *D. simulans* lineages are measured relative to a reconstructed ancestor (see Methods).

### Comparing *D. simulans* assemblies

Our assembly (hereafter  $Dsim_{w501}$ ) offers significant improvements over the previous assembly (hereafter  $Dsim_{ref}$ ) (Begun et al. 2007; *Drosophila* 12 Genomes Consortium et al. 2007) in several fundamental ways that are crucial to confidence in genome sequence accuracy. First, we effectively increase the assembly length across all chromosome arms by  $\sim 17\%$  on average (Supplemental Fig. 5; Table 1). The largest improvement in sequence content over  $Dsim_{ref}$  is for the X chromosome. In particular, our assembly produces an additional 6.41 Mb on the X chromosome, which is 44% larger than  $Dsim_{ref}$  (Table 1). A pairwise dotplot comparing  $Dsim_{w501}$  to the *D. melanogaster* and  $Dsim_{ref}$  assemblies reveals that these gains are widely dispersed across the X chromosome rather than localized to a few regions (Fig. 1). The substantial increase in coverage of the X chromosome translates to a 17% gain in the total number of full-length orthologous gene matches (Supplemental Table 5). We also see particularly large gains in the assembly length compared with  $Dsim_{ref}$  on chromosome 4. Like the X, the additional coverage is widely dispersed rather than localized (see the inset of Supplemental Fig. 5). Second,  $Dsim_{w501}$  contains fewer misassembled regions than  $Dsim_{ref}$  (Supplemental Table 6), and our assembly properly conforms with the inferred genetic ordering of markers (Supplemental Fig. 6), at the level of resolution permitted by previously published linkage data (Andolfatto et al.

2011a). In particular, several large misassemblies detected using genetic linkage patterns and compiled from the GFF (Gene Format File) for  $Dsim_{ref}$  (see Tables S9.1 and S9.2 of Andolfatto et al. 2011a) are not detected in  $Dsim_{w501}$  (Supplemental Table 6). In addition, we detect an inversion on the X chromosome (X:13361146–13723239) in  $Dsim_{ref}$  relative to our assembly ( $Dsim_{w501}$ ) that is also not found in *D. melanogaster* (Fig. 1). Support from paired-end reads at both putative breakpoints suggest that this inversion is the result of a misassembly in  $Dsim_{ref}$ .

Third, because  $Dsim_{ref}$  is a mosaic assembly of six inbred strains sequenced to relatively low coverage, we expect that  $Dsim_{w501}$  should contain fewer sequencing errors since it is based on high sequence coverage of a single inbred strain. By comparing orthologs of *D. melanogaster* protein-coding genes between the two *D. simulans* assemblies (see Methods), we find that  $Dsim_{w501}$  contains fewer predicted proteins with frameshift mutations (6.6% vs. 20.6%) and premature stop codons (4.0% vs. 5.9%) while containing more informative non-N codons (6,322,536 vs. 5,698,459) and a greater proportion of genes with intact start and stop codons (94.1% vs. 85.8%) (Fig. 2; Supplemental Table 5). The high fraction of *D. simulans* orthologs with frameshifts in both assemblies represents difficulties in creating multiple sequence alignments that preserve proper gene structure (intron–exon boundaries) in all three species. Because site classification by annotation is with respect to the *D. melanogaster* annotation, we find a similarly high fraction of frameshifts in the *D. yakuba* ortholog (14.2% using  $Dsim_{w501}$  and 13.9% using  $Dsim_{ref}$ ). Furthermore, while the fraction of genes with a premature stop codon in  $Dsim_{w501}$  is similar with respect to that found in the *D. yakuba* ortholog (4.0% vs. 3.8%), an increase is found in  $Dsim_{ref}$  (4.9% vs. 3.7%). The reduced number of inferred frameshifts and premature stop codons using the *D. melanogaster* annotation point to higher sequence quality in  $Dsim_{w501}$ .

Analysis of  $Dsim_{w501}$  also results in systematically lower divergence estimates for the *D. simulans* lineage in comparison to  $Dsim_{ref}$  across all site classes, regardless of chromosomal context (Supplemental Fig. 9; Table 2). In Figure 3, we show that divergence measured using  $Dsim_{ref}$  is biased upward relative to  $Dsim_{w501}$  when divergence estimates differ for the *D. simulans* branch (i.e., estimates from  $Dsim_{ref}$  are more often greater than estimates from  $Dsim_{w501}$ ). In contrast, divergence estimates along the *D. melanogaster* lineage are not biased by the choice of *D. simulans* reference. These patterns suggest a systematic overestimation of the *D. simulans* branch length in analyses using  $Dsim_{ref}$ .

Finally, as an additional evaluation of quality, we consider the spatial clustering of amino acid substitutions in protein sequences (Callahan et al. 2011). In examining the spatial pattern of coding sequence substitutions within and between seven *Drosophilid* genomes, Callahan et al. (2011) found an excess of intralocus clustering of nonsynonymous substitutions over a physical scale of about 20 codons. Callahan et al. (2011) specifically identify *D. simulans* as an outlier in their analyses, citing the *D. simulans* reference sequence quality as a possible cause. In support of this claim, we show that the extent of intralocus

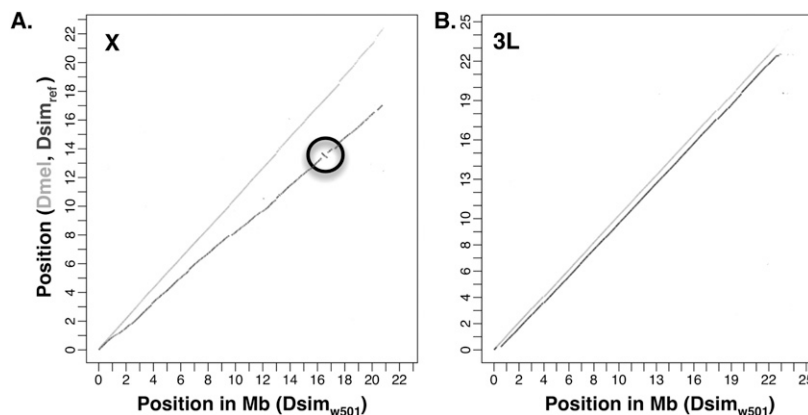


**Figure 1.** Dotplot for chromosomes X (A) and 3L (B) comparing our assembly to that of *D. melanogaster* (light gray) and *D. simulans* reference assembly (dark gray) (Begun et al. 2007). An inversion on the X (circled) is an example of a misassembly detected in the Begun et al. (2007) *D. simulans* assembly spanning X:13361146–13723239.

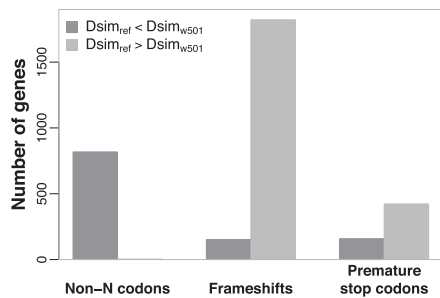


**Figure 2.** Sequence quality metrics by gene. The number of *D. simulans* orthologs for which the amount of informative non-N codons, frameshifts, and premature stop codons generated from  $D_{sim\_ref}$  differs from  $D_{sim\_w501}$  (in total, 11,053 genes are compared).

spatial clustering found in  $D_{sim\_w501}$  is similar to that found in the *D. melanogaster* lineage (Fig. 4), and *D. simulans* no longer remains an outlier with respect to the intralineage clustering excess (Fig. 4, inset).

### Faster evolution in the *D. melanogaster* lineage

Table 2 and Figure 5 catalog rates of divergence along the *D. melanogaster* and *D. simulans* lineages for various site annotation categories. The rank order of rates of divergence across site annotation classes is the same in both *D. melanogaster* and *D. simulans*, consistent with previous findings; bases 8–30 of introns shorter than 100 bp (hereafter, intron<sub>FEI</sub> sites) evolve the fastest, and non-synonymous sites the slowest (Halligan and Keightley 2006; Parsch et al. 2010). Based on levels of nucleotide diversity, *D. simulans* is predicted to have a somewhat larger historical  $N_e$  than that of *D. melanogaster*. As a result, rates of evolution are predicted to be faster along the *D. melanogaster* lineage due to the increased role of random genetic drift and corresponding lower efficacy of selection for species with smaller  $N_e$ . For the major autosomes (including only major arms 2L, 2R, 3L, and 3R for all subsequent analyses) and the X chromosome, we find that divergence along the *D. melanogaster* lineage is indeed faster than *D. simulans* across all annotated site classes, apparent in the distribution of rates of divergence across genes and nonoverlapping 50-kb windows (Fig. 5; Supplemental Fig. 9; Table 2).

We note that intron<sub>FEI</sub> sites also evolve 16%–20% faster in the *D. melanogaster* lineage. Assuming that these sites are neutral, this raises the possibility that there may be a mutation rate difference between the two species. Such a difference in mutation rates need not involve a mutation rate difference per generation but may simply reflect a different average historical generation time for the two species. While differences in mutation rate may be a contributing factor to the generally higher divergence along the *D. melanogaster* lineage, the extent of the divergence excess varies significantly across site annotations ( $P = 7.34 \times 10^{-52}$  for autosomes,  $P = 1.22 \times 10^{-12}$  for the X; Kruskal-Wallis test), suggesting that between-lineage mutation rate differences alone cannot fully account for the acceleration in the *D. melanogaster* lineage.

Heterogeneity in levels of divergence across site annotation classes would be expected if the two species differed in  $N_e$  and thus were subject to different intensities of selective constraint (see Discussion). Assuming that intron<sub>FEI</sub> sites are neutral, we can quantify constraint across site classes as  $1 - \frac{D_{annot}}{D_{intron\_FEI}}$ . For both non-coding and synonymous sites, we find that constraint is stronger in *D. simulans* on the autosomes, while this trend is weaker on the

X chromosome ( $P > 0.02$  for X,  $P < 1 \times 10^{-5}$  for autosomes; Sign Test). Interestingly, however, we find the reverse pattern for non-synonymous sites, where constraint is instead significantly higher in *D. melanogaster* ( $P = 0.005$  for X,  $P = 0.0026$  for autosomes; Sign Test). Assuming that intron<sub>FEI</sub> sites are, indeed, neutral, the discord among site annotations is inconsistent with a model that posits that most divergence is neutral or slightly deleterious. This implies that either positive selection contributes substantially to divergence or that intron<sub>FEI</sub> sites themselves are constrained and subject to different intensities of selection in the *D. melanogaster* and *D. simulans* lineages.

### X versus autosome evolution

Comparing divergence rates between the X chromosome and autosomes provides an opportunity to examine the nature of newly arising mutations and the substitutions that accumulate between species (Charlesworth et al. 1987). Because the rate of neutral evolution is solely dependent on the mutation rate, the X should evolve at the same rate as the autosomes at neutral sites, assuming that mutation rates are equal. However, due to hemizyosity in males, all newly arising non-neutral mutations on the X, including those that are recessive, are exposed to natural selection (assuming that selection is not female specific). As a result, if a substantial fraction of newly arising non-neutral mutations is partly recessive, the X is expected to fix more beneficial substitutions than autosomes (the “faster-X” effect), and the converse pattern (i.e., a “slower-X”) is expected for detrimental substitutions. The net effect on rates of evolution for the X versus the autosomes depends on a balance between the fraction of substitutions accumulating between species that are beneficial, neutral, and detrimental.

Notably, the X/A (X-to-autosome) ratio is close to unity for intron<sub>FEI</sub> sites, which have been proposed to be close to a neutrally evolving class of sites in the *D. melanogaster* genome (Halligan and Keightley 2006; Parsch et al. 2010). A priori, we expect that sites under pervasive negative selection (i.e., most sites in the *Drosophila* genome) (Andolfatto 2005; Halligan and Keightley 2006; Haddrill et al. 2008) should accumulate substitutions more slowly on the X, due to the more efficient selection expected on this chromosome. Contrary to this expectation, we find strong evidence for faster-X divergence among 5′ and 3′ UTRs, intron >100 sites, and faster-X divergence at nonsynonymous sites in

**Table 2.** Lineage-specific divergence by annotation and chromosomal context in *D. simulans* and *D. melanogaster*

Annotation	Chromosome	$D_{Dsim}$	$D_{Dmel}$	$D_{Dmel}/D_{Dsim}$
Nonsyn <sub>of</sub>	X	0.00655	0.00637	1.01869
	2 + 3	0.00583	0.00642	1.06721
Syn <sub>4f</sub>	X	0.03870	0.05383	1.39243
	2 + 3	0.04334	0.05575	1.29182
Intron <sub>FEI</sub>	X	0.05837	0.06961	1.20684
	2 + 3	0.05794	0.06727	1.16338
Intron <sub>&gt;100bp</sub>	X	0.03398	0.04150	1.23406
	2 + 3	0.03008	0.03826	1.29681
5′ UTR	X	0.02159	0.02719	1.24987
	2 + 3	0.01743	0.02341	1.32632
3′ UTR	X	0.02150	0.02684	1.23197
	2 + 3	0.01553	0.02076	1.30797

Divergence estimates from the shared ancestor of *D. simulans*/*D. melanogaster* are reported (median across 50-kb windows). Refer to Table 1 of Begun et al. (2007) to compare  $D_{sim\_ref}$  rates, and see Supplemental Figure 9 for statistical tests of  $D_{mel}/D_{sim}$  divergence ratios being >1.

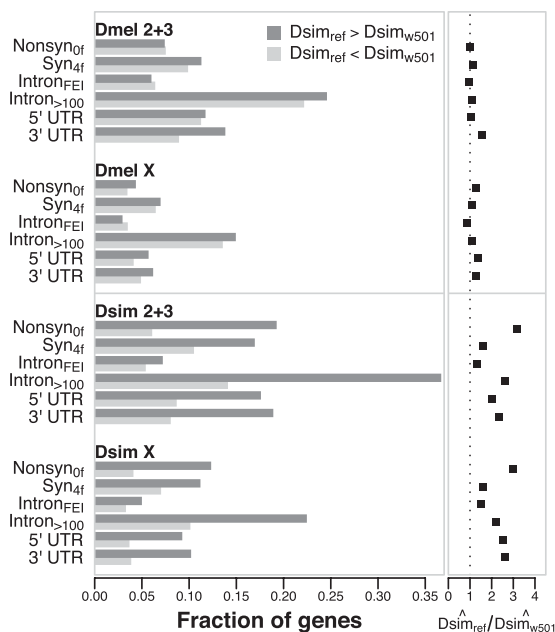


**Figure 3.** Comparison of estimated lineage-specific divergence rates using the two *D. simulans* assemblies. The fraction of genes, by chromosome and site class, for which the estimated divergence rate per gene is different (greater or less than) depending on the *D. simulans* assembly used. Estimated rates for *D. melanogaster* are shown on top and *D. simulans* on bottom. (Right) The ratio of the number of genes for which the estimate from  $Dsim_{ref} > Dsim_{ws01}$  relative to  $Dsim_{ref} < Dsim_{ws01}$ . Note that putatively neutral intron<sub>FEI</sub> sites correspond to bases 8–30 of introns shorter than 100 bp (Halligan and Keightley 2006; Parsch et al. 2010).

both *D. simulans* and *D. melanogaster* (Fig. 6; Table 2; Supplemental Table 7). The faster-X pattern for these site classes is consistent with the more frequent fixation of beneficial mutations arising on the X chromosome, where a large fraction of the UTR, intron, and nonsynonymous divergence (i.e., >50%) along the *D. simulans* and *D. melanogaster* lineages is inferred to be the product of positive selection (Andolfatto 2005; Haddrill et al. 2008). While a faster-X seems apparent for many site classes, we conversely find evidence for a slower-X at synonymous sites, where a large fraction of the divergence accumulating at synonymous sites in the two species is instead inferred to be weakly detrimental (Supplemental Table 9; Akashi 1995; Begun 2001). Of note, the dramatic discrepancy in rates of evolution on the X and autosomes (Fig. 6) is not apparent when comparing between autosomes 2 and 3 (Supplemental Fig. 11; Supplemental Table 8).

Interestingly, the magnitude of the bias in the X/A ratio appears more pronounced in *D. simulans* relative to *D. melanogaster* across all site classes, and the two distributions are significantly different (Fig. 6,  $P < 2.2 \times 10^{-16}$  for all site classes; Wilcoxon Test, unpaired). The “faster” faster-X pattern in *D. simulans* suggests that a larger proportion of newly arising mutations are beneficial in *D. simulans* (as weaker purifying selection in the *D. simulans* lineage seems less likely). On the other hand, the “slower” slower-X pattern for synonymous sites in *D. simulans* conforms with expectations of stronger codon usage bias reported in *D. simulans* than *D. melanogaster* (Akashi 1995; Akashi and Schaeffer 1997; McVean and Vieira 2001; Nielsen et al. 2007; Andolfatto et al. 2011b).

While it is tempting to interpret differences in rates of evolution on the X and autosomes in the context of the dominance/

recessivity of newly arising mutations, this phenomenon does not preclude alternative explanations (Vicoso and Charlesworth 2006). In particular, the same pattern could arise simply from differences in gene composition on the X versus the autosomes (i.e., the “different X” hypothesis). To evaluate the “different X” explanation for differential rates of divergence on the X versus autosomes, we carried out an ANOVA analysis that incorporates Gene Ontology (GO) as a factor (see Methods). We find that GO is a significant predictor of rates of divergence across all classes of sites (Supplemental Table 10). Interestingly, the trend toward a faster-X at nonsynonymous sites in *D. simulans* and *D. melanogaster* (Fig. 6; Supplemental Table 7) is no longer significant when accounting for GO category (Supplemental Table 10). This suggests that a large part of the faster-X effect for nonsynonymous sites may be explained solely by differences in gene composition on the X and autosomes. Notably, we find no effect of chromosome 2 linkage when restricting the analysis to autosomes, suggesting the X–autosome difference is distinct from more general genomic heterogeneity due to GO category (Supplemental Table 12). This said, X-linkage is still a significant predictor of divergence at synonymous and noncoding sites even after accounting for GO category, suggesting that the differences in gene composition cannot fully account for X–autosome differences (Supplemental Table 10).

Related to the possibility of gene composition differences discussed above is the issue of differences in gene expression patterns between males and females for genes on the X and autosomes. Controlling for sex-biased expression patterns is particularly interesting because the X chromosome is deficient in male-biased genes (Sturgill et al. 2007; Zhang et al. 2007). Since proteins with male-biased expression tend to evolve faster (Zhang et al. 2007), this could obscure a faster-X effect due to recessive beneficial substitutions at nonsynonymous sites. To evaluate this possibility, we performed an ANOVA analysis incorporating sex-biased expression data measured in *D. melanogaster* (Gnad and Parsch 2006) (see Methods). In general, we find that sex-biased expression is a significant predictor of rates of divergence across most classes of sites in both lineages (Supplemental Table 11). Interestingly, however, we find that even after accounting for sex-biased expression patterns, X-linkage remains a significant factor predicting rates of divergence at most classes of nonintronic sites in both species (Supplemental Table 11). Similar to the GO analysis (above), restricting the analysis to autosomes fails to reveal any significant effect of chromosome 2 linkage, suggesting that X–autosome differences are distinct from more general genomic heterogeneity correlated with sex-biased expression patterns (Supplemental Table 13).

## Discussion

The first genome-wide study comparing rates of evolution between *D. melanogaster* and *D. simulans* was based on a mixed-sex, multiple-strain, low-coverage genome assembly of *D. simulans* versus the *D. melanogaster* reference assembly (Begun et al. 2007). That analysis revealed several complex patterns of lineage-specific divergence that were difficult to interpret in the context of population genetic models that considered the effects of differences in  $N_e$  and genomic context. When comparing genomes of species that differ in sequence coverage and quality, complicated and unreliable patterns may emerge specific to the species whose genome sequence suffers from lower quality. In particular, we expect that divergence will generally be overestimated for the species with

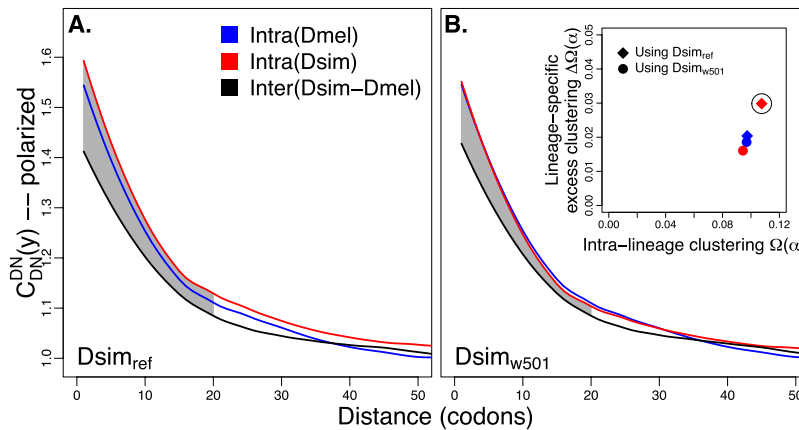


**Figure 4.** Comparison of intralineage and interlineage clustering of nonsynonymous substitutions. For all comparisons,  $C_{DN}^{DN}(Y)$  (the correlation in divergence between nonsynonymous substitutions) decreases with increasing distance separating two nonsynonymous substitutions, specific to the lineage from which the substitution arose (polarized), following Figure 4A of Callahan et al. (2011). The amount of intralineage clustering within *D. simulans* (red line) and *D. melanogaster* (blue line) relative to interlineage clustering (black line) is shown separately for the two *D. simulans* assemblies:  $Dsim_{ref}$  (A);  $Dsim_{w501}$  (B). The excess of intralineage relative to interlineage clustering in *D. simulans* is represented by the area between the red and blue curves for the first 20 codons [ $\Delta\Omega(\alpha)$ , shaded in gray]. Note that the same set of genes from both assemblies is analyzed, and *D. simulans* orthologs from either assembly containing a premature stop codon or non-start or stop codons are excluded. (B) Unlike the pattern from  $Dsim_{ref}$ , a similar amount of intralineage clustering is found in both the *D. simulans* and *D. melanogaster* lineages when using  $Dsim_{w501}$  (greater overlap between blue and red lines; shaded region in gray is smaller). The intralineage clustering excess  $\Delta\Omega(\alpha)$  relative to the extent of intralineage clustering  $\Omega(\alpha)$  is shown in the inset (following Fig. 4B of Callahan et al. 2011). A considerably larger intralineage clustering excess is found in the *D. simulans* lineage when using  $Dsim_{ref}$ , which is also circled in the inset.

lower genome quality. Sequence errors may be particularly problematic when the evolutionary distance between the studied species is small, such that the proportion of the divergence they represent will be larger. Similarly, one might be apprehensive of overinterpreting patterns that emerge from intragenomic studies where sequence coverage and quality differ between chromosomes, such as those examining the evolutionary consequences of chromosomal context.

To address these concerns, we created an improved version of the *D. simulans* genome that is based on high coverage of a single strain and, by sequencing females only, has close to equal coverage on the X and autosomes. By several metrics, our efforts have resulted in an assembly with fewer sequence and assembly errors than the previous *D. simulans* reference assembly. The scaffolding of our genome assembly was guided by the *D. melanogaster* genome reference and is expected to be biased by this (particularly in terms of unique genomic content). However, we expect that gains from an independent assembly of contigs would mostly lie in heterochromatic regions, and these regions would not contribute much to the evolutionary analysis because they would also be difficult to align between species due to their repetitive nature. Our evolutionary analysis is also limited by the number of full-length orthologs found in the *D. yakuba* genome reference, and improvements to the *D. yakuba* genome could increase the total number of gene orthologs analyzed. While our assembly greatly reduces the number of frameshifts and premature stop codons compared with the previous assembly, we note that this issue still affects almost 9% of gene alignments (and were excluded from further analyses). This may in large part be caused by our reliance on gene structure annotations defined in *D. melanogaster*, an issue common to evolutionary comparisons to model organisms. This problem could be remedied to some extent by a community effort

to independently annotate *D. simulans* and *D. yakuba*, which would allow for more independent comparisons of orthologs in the three species.

Caveats aside, our analyses reveal a different portrait of lineage-specific divergence patterns in *D. melanogaster* and *D. simulans* than the analysis of the original *D. simulans* assembly (Begun et al. 2007). Differences in the pattern of lineage-specific divergence in two species can be interpreted through theoretical predictions of population genetic models that consider the dynamics of slightly deleterious mutations in the context of differences in  $N_e$  (Ohta 1973; Charlesworth et al. 1993; Akashi 1995; Charlesworth 2009). In particular, the fate of slightly deleterious mutations occurring in species with large  $N_e$  is predicted to be more efficiently removed by natural selection, whereas in species with smaller  $N_e$ , a larger fraction of these mutations can instead be fixed by random genetic drift. Of the two species, *D. simulans* is believed to have had the historically larger  $N_e$  based on comparisons of levels of nucleotide diversity and from patterns of codon usage bias (Aquadro et al. 1988; Akashi 1995; Moriyama and Powell 1996; Andolfatto 2001; Andolfatto et al. 2011b). Our finding of generally lower rates of divergence in *D. simulans* is broadly consistent with this view. Moreover, a difference in  $N_e$  between the two species is also supported by our finding of significant heterogeneity across site classes in the extent to which *D. melanogaster* evolves faster than *D. simulans*. Our interpretation of this pattern is that, because the distribution of fitness effects of newly arising mutations varies among annotation site classes (Eyre-Walker and Keightley 2007), we therefore expect the fraction of sites subject to nearly neutral dynamics to similarly differ across site class (with the largest frac-

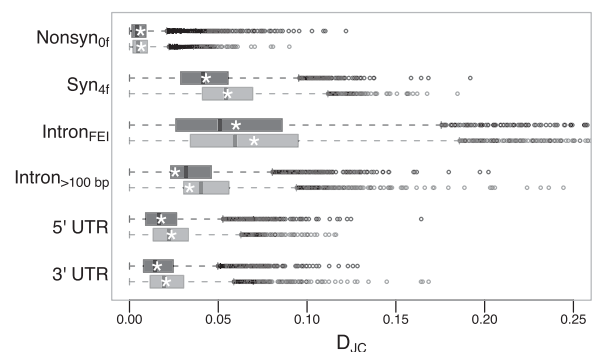


**Figure 5.** Boxplot distribution of lineage-specific divergence by gene across different site classes in autosomal (2 + 3) genes in *D. simulans* and *D. melanogaster*. For each site class, the top darker bar represents the distribution across *D. simulans*, and the bottom lighter bar for *D. melanogaster* (each gene must contain a minimum of 10 non-N sites for intron<sub>FEI</sub> sites and 100 otherwise). (\*) The weighted average (based on the number of sites corresponding to the annotated class for each gene) across all genes. See also Table 2.

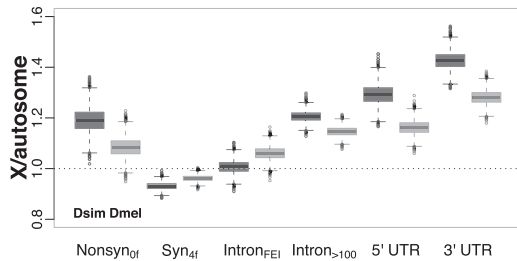


**Figure 6.** X/autosome divergence ratio in *D. simulans* and *D. melanogaster*. The X/A divergence ratio is expected to be unity assuming that the X and autosomes have the same effective population size in the ancestor of these species. In support of this, synonymous nucleotide diversities on the X and autosomes are approximately equal in African populations of both species (Andolfatto 2001). The distribution for X/autosome divergence ratios reflects 10,000 bootstrap samples with replacement by gene across the various site classes, separately for genes on the X and autosomes. Refer to Supplemental Table 7 for bootstrap *P*-values.

tion expected for synonymous and potentially intron<sub>FEI</sub> sites, if the latter are also nearly neutral).

This said, we have also shown that intron<sub>FEI</sub> sites, believed to be close to neutrally evolving (Halligan and Keightley 2006; Parsch et al. 2010), exhibit faster rates of divergence in the *D. melanogaster* lineage. One possible explanation for this pattern is a difference in mutation rate in the *D. melanogaster* and *D. simulans* lineages, perhaps as the result of a subtle difference in average generation time. However, by assessing levels of “constraint” at nonsynonymous sites using intron<sub>FEI</sub> sites as a neutral reference, we find that constraint at nonsynonymous sites is instead higher in *D. melanogaster* than in *D. simulans*. In other words, while divergence is greater in *D. melanogaster* for both nonsynonymous sites and intron<sub>FEI</sub> sites, the ratio of rates at nonsynonymous relative to intron<sub>FEI</sub> sites is smaller than in the *D. simulans* lineage. From the perspective that most of genome evolution is due to the accumulation of neutral and slightly deleterious mutations, this suggests that intron<sub>FEI</sub> sites themselves may be subject to weak purifying selection at the nucleotide level, and that the intensity of this selection is weaker in *D. melanogaster*. This finding is not actually inconsistent with current analyses of polymorphism data to date, which has so far been restricted to a small sample of genomic regions surveyed in *D. melanogaster* (Parsch et al. 2010).

An alternative, although not mutually exclusive, explanation is that a substantial fraction of lineage-specific divergence is the product of positive selection. In fact, several studies based on an analysis of polymorphisms and divergence have suggested that a large fraction of divergence in the *D. melanogaster* and *D. simulans* lineages, particularly at nonsynonymous sites, is in excess of neutral expectations (Fay et al. 2002; Smith and Eyre-Walker 2002; Haddrill et al. 2008; Andolfatto et al. 2011b; Wilson et al. 2011). If this divergence excess is the product of recurrent positive selection, we expect more rapid evolution (and correspondingly less constraint) in *D. simulans* if it indeed has had a larger  $N_e$ . Faster rates of nonsynonymous substitution in *D. simulans*, particularly on the X, may also reflect a difference in the beneficial mutation rate in the two species. Interestingly, Wilson et al. (2011) estimate that the rate of newly arising nonsynonymous mutations that are moderately to strongly beneficial is almost threefold higher in *D. simulans* than in *D. melanogaster*.

Importantly, our assembly allows for a more quantitative comparison between rates of evolution on the X chromosome

versus the autosomes. In contrast to the study of Begun et al. (2007, see their Table S3), we find that the X chromosome evolves significantly faster than autosomes for most noncoding sites and significantly slower for synonymous sites in both species. Notably, we find that the X/autosomes ratio for intron<sub>FEI</sub> sites is close to 1 in both species, and synonymous sites evolve slower on the X relative to autosomes (Fig. 6). Begun et al. (2007) note that hypertranscription of the X in males may contribute to an elevated mutation rate. However, since both intron<sub>FEI</sub> and synonymous sites are transcribed on the X, the hypertranscription-associated mutation rate increase on the X explanation seems less plausible in explaining the faster-X pattern. Consequently, the faster-X pattern is more likely explained by population genetic models invoking selection. Several previous studies have interpreted the faster-X pattern as reflecting an accumulation of recessive beneficial mutations on the X relative to autosomes, due to more efficient positive selection in males (Vicoso and Charlesworth 2006). By considering the effects of Gene Ontology and sex-biased expression, we conclude that the trend toward a faster-X for nonsynonymous sites is likely to be largely explained by differences in gene composition on the X versus the autosomes. This said, GO category and sex-biased expression fail to account for the faster-X pattern observed at 3' UTRs (or the slower-X for synonymous sites), although we have not explored all possible factors (e.g., expression level, breadth of expression, etc.).

Our results highlight the importance of genome quality on the quality of the evolutionary inferences that can be drawn from low coverage genomes. Among the 12 sequenced *Drosophila* genomes (*Drosophila* 12 Genomes Consortium et al. 2007), *D. simulans* had the lowest coverage (Q20 coverage 2.9); however, similar issues may plague analyses involving other low-coverage *Drosophila* genomes (e.g., *Drosophila sechellia*, Q20 coverage 4.9; and *Drosophila persimilis*, Q20 4.1). Our results also have implications for a large number of ongoing projects (e.g., the Genome 10K Project [<http://www.genome10k.org>]; the *Drosophila* Genetic Reference Panel [DGRP] [Mackay et al. 2012]; the Human 1000 Genomes Project [The 1000 Genomes Project Consortium 2010]; and the 1001 Genomes Project in *Arabidopsis thaliana* [Cao et al. 2011]) that aim to survey a large number of genomes at relatively low coverage or perform analyses comparing genomes or genomic regions that vary substantially in coverage. Our results also highlight how studies examining the evolutionary consequences of chromosomal context can depend on heterogeneity in coverage among genomic regions (in our case, X vs. autosome). Such concerns may also apply to analyses comparing high and low recombining and heterochromatic regions, if the latter are associated with lower coverage. Given that poor genome quality can both obscure interesting evolutionary patterns, as well as create spurious ones, we may stand to learn more from fewer deeply sequenced genomes than a large number of low-coverage genomes.

## Methods

### Sequencing and assembly

We constructed a standard Illumina paired-end genomic DNA library for *D. simulans* females of strain  $w^{501}$  following the manufacturer's instructions (<http://www.illumina.com>). Genomic DNA was isolated using standard protocols and sheared to a mean size of 500 bp using a Covaris sonicator. We collected 124 million paired-end 104-bp and 101-bp reads by running this library on two different sequencers (Supplemental Table 1). Before assembly, our Illumina reads were error-corrected using Quake (Kelley et al. 2010)

with a  $k$ -mer of size 17. We combined these data with previously published Sanger sequence data (Begun et al. 2007) and created a de novo assembly using Velvet version 1.1.04 (Zerbino and Birney 2008). Due to limitations in Velvet, the 3-kb insert plasmid paired-end reads were run with the `-longPaired` option while all 40-kb insert fosmid reads were treated as single long reads (`-long`). Our best assembly used a  $k$ -mer of 65 (as determined by the VelvetOptimiser script) and comprised 21,613 contigs totaling 123,899,117 bp with an  $N_{50}$  of 150 kb (Supplemental Table 2).

Ordering and placement of Velvet contigs were determined first by MUMmer version 3.23 (nucmer and show-coords) (Kurtz et al. 2004) against a “TE-minimized” version of the *D. melanogaster* genome (FlyBase release r5.33), where all annotated transposable elements were excised (Supplemental Fig. 3). The reduced *D. melanogaster* genome totaled 113,815,635 bp across chromosomes X, 2L, 2R, 3L, 3R, and 4. The mtDNA was treated separately and assembled relative to the *silI* haplotype, based on similarity of Velvet contigs to each of the three *D. simulans* mtDNA haplotypes (GenBank accession numbers NC 005781, AF200845, AF200847) (Ballard 2000). To avoid complications with repetitive elements, nonuniquely mapping contigs and those engulfed by larger uniquely mapped contigs were set aside (unincorporated-contigs.fa). Three contigs appeared to be chimeric and were split apart and reincorporated separately. The final ordered set of 2156 contigs were stitched together with a 100-bp buffer of Ns. We visually inspected the placement and ordering of contigs, against the *D. melanogaster*, *D. simulans*, and *D. yakuba* reference genomes (FlyBase versions r5.33, r1.3 and r1.3) with MUMmer (Kurtz et al. 2004). Following the stitching of ordered contigs, we mapped all uncorrected reads against this initial assembly with BWA (Li et al. 2009) for the Illumina short reads and Sanger unpaired long reads and SSAHA2 version 2.5.4 (Ning et al. 2001) for the Sanger paired long reads. Inspection of the mapped reads was summarized by creating a vcf file with samtools mpileup and bcftools version 0.1.18 (Li et al. 2009). The assembly was then updated with single-nucleotide and insertion/deletion variants (Q20 for substitutions and 50 for indels) using the vcfutils.pl vcf2fq tool from SAMtools. Three iterations of assembly updating by remapping of reads resulted in minor improvements in the total number of paired-reads mapped.

### Transposable elements

A total of 5142 (of 5425) annotated transposons in *D. melanogaster* had at least one BLAT match (tblatx) (Kent 2002) to at least one of 10,484 contigs (Supplemental Fig. 1A). The total sequence across all contigs that matched transposable elements was 6.85% of the total assembly length. Full-length transposon matches to contigs were biased toward short transposons. With respect to TE presence among contigs of varying lengths, we found that most contigs  $\leq 500$  bp fully resembled *D. melanogaster* transposons in comparison to larger contigs (Supplemental Fig. 1B). For the larger contigs, repetitive elements did not appear to be the only factor limiting the assembly because their presence is not biased toward the ends of contigs (Supplemental Fig. 2).

### *D. melanogaster*–*D. simulans*–*D. yakuba* gene alignments

Because gene structures are better annotated in the *D. melanogaster* reference assembly, we transferred gene annotations from the *D. melanogaster* genome to both *D. simulans* and *D. yakuba* through multiple sequence alignments containing all three orthologs. Each protein-coding gene in *D. melanogaster* (FlyBase release r5.33, dmel-all-gene-r5.33.fasta) was first BLAT-ed (Kent 2002) against both *D. simulans* assemblies and the *D. yakuba* assembly (FlyBase

version r1.3) to identify putative orthologs. Chromosome 4 was generally excluded from autosome analysis due to low gene content. We only examined gene alignments where all orthologs were  $< 50,000$  bp (to avoid memory complications with multiple sequence alignment programs) and spanned at least 50% of the *D. melanogaster* transcript. The resulting BLAT hits were filtered to identify the best and unique hit (based on longest and highest percent sequence identity).

In an effort to preserve the CDS-exon structure as dictated by the *D. melanogaster* annotation, we aligned the entire *D. melanogaster* transcript with both *D. simulans* and *D. yakuba* BLAT hits with FSA version 1.15.6 with the `refalign`, `exonerate`, and `softmasked` parameters enabled (Bradley et al. 2009) followed by a profile alignment with a padded CDS sequence representing the union of coding regions across all *D. melanogaster* isoforms using a profile alignment with MUSCLE v3.8.31 (Edgar 2004). We converted out-of-frame deletions (with respect to the *D. melanogaster* annotation) whose lengths are multiples of 3 into full codon deletions by repositioning the bases corresponding to the disrupted codon relative to the first aligned codon position in the resulting multiple sequence alignment.

For our analyses, we created a set of genes for which we have higher confidence that the gene structure is the same in all three species. To do this, we ensured that alignments are free of premature stop codons and frameshifts in the *D. simulans* sequence. The restriction was not extended to *D. yakuba* since we are only interested in rates of evolution in the *D. melanogaster* and *D. simulans* branches and only rely on *D. yakuba* to reconstruct the ancestral state. From the resulting *D. simulans*–*D. melanogaster*–*D. yakuba* multiple sequence alignment, the ancestor corresponding to *D. simulans*–*D. melanogaster* was reconstructed separately for coding (codeml; RateAncestor=2, model=1) and non-coding (baseml; RateAncestor=2, model=4) regions using PAML version 4.4c (Yang 2007). The final number of protein-coding genes analyzed is reported in Supplemental Table 5.

For each protein-coding gene, we select the isoform with the highest content of protein-coding sites. For regions overlapped by other isoforms and/or genes, we classify each site according to the following hierarchy:  $\text{intron}_{\text{FEI}}$ ,  $\text{intron}_{>100}$ , 5' UTR, 3' UTR, followed by CDS (highest). Thus, if a site resides in an  $\text{intron}_{>100}$  in one gene and CDS for another, the site is classified as CDS. For gene-based analyses, we use all sites corresponding to each site class that are within the boundaries of the gene. For window-based analyses, we exclude genes spanning multiple windows and require a minimum of 100 sites for which the ancestral state was reconstructed for all annotations analyzed with the exception of  $\text{intron}_{\text{FEI}}$  sites, where we require a minimum of 10 sites.

### Evolutionary analyses

After all sites are partitioned into the above annotation categories, all evolutionary analyses are performed with Polymorphorama (Hadrill et al. 2008). Counts of nonsynonymous (nondegenerate) and synonymous (fourfold) sites and the classification of nonsynonymous, synonymous, and P/U codon substitutions are performed with Polymorphorama. Preferred/unpreferred codons are classified based on the codon preference table from Vicario et al. (2007). To correct for multiple hits, we report divergence estimates with the Jukes–Cantor correction (Jukes and Cantor 1969). To correct for mutation biases and base composition, we correct divergences for “mutational opportunity” (Petrov and Hartl 1999) by measuring the rate of each of the 16 types of base substitution from the reconstructed ancestor observed at  $\text{intron}_{\text{FEI}}$  sites (Supplemental Table 14). We detected significant heterogeneity between  $\text{GC} \rightarrow \text{AT}$  and  $\text{AT} \rightarrow \text{GC}$  substitutions in all four contexts (Fisher’s

exact test,  $P < 2.2 \times 10^{-16}$  between *D. melanogaster* and *D. simulans* for both the X and autosomes;  $P = 6.872 \times 10^{-8}$  between the X and autosomes for *D. melanogaster*; and  $P = 0.001889$  between the X and autosomes for *D. simulans*) and thus generated a separate table for each context. Depending on the context, we used one of these tables as a proxy for the scaled mutation rate at a given site that depends on the inferred state (A, G, C, or T) in the reconstructed ancestor.

### Gene Ontology and sex-biased expression analyses

Each annotated *D. melanogaster* protein-coding gene was classified by Gene Ontology according to the top-level molecular function terms of GO:0003674; GO:0001071; GO:0003824; GO:0005198; GO:0005215; GO:0005488; GO:0009055; GO:0016015; GO:0016209; GO:0016247; GO:0016530; GO:0030234; GO:0030528; GO:0031386; GO:0045182; GO:0045735; and GO:0060089. GO terms for all genes were assigned using map2slim.pl (go-perl module) according to ftp.flybase.net/releases/FB2011\_01/precomputed\_files/ontologies/gene\_ontology.obo.zip.

Before testing for an X-effect, a stepwise regression (R function “step”) was used to identify significant GO terms for each site class, based on Akaike’s Information Criterion. With respect to sex-bias classification by gene expression, we used data prepared in the Sebida database (<http://www.sebida.de>, sebida\_melanogaster\_3.0.txt) (Gnad and Parsch 2006). Only genes with false-discovery rates  $< 0.01$  were included. We compared the alternative model fits with the ANOVA function in R to test for effects by gene function, sex-biased expression, and X-linkage on divergence rates.

### Data access

The raw short read data generated from this study have been submitted to the NCBI Sequence Read Archive (SRA) (<http://www.ncbi.nlm.nih.gov/sra>) under accession number SRA055460. The *D. simulans* *w*<sup>501</sup> assembly is available at <http://genomics.princeton.edu/AndolfattoLab/Links.html>.

### Acknowledgments

We thank Molly Przeworski and David Stern for useful discussions and Ying Zhen for useful comments. We also thank Stephen Wright for use of his server to run the Velvet assembly. This work was funded in part by NIH grant R01-GM085183 to K.R.T. and R01-GM083228 to P.A.

### References

The 1000 Genomes Project Consortium. 2010. A map of human genome variation from population-scale sequencing. *Nature* **467**: 1061–1073.

Akashi H. 1995. Inferring weak selection from patterns of polymorphism and divergence at “silent” sites in *Drosophila* DNA. *Genetics* **139**: 1067–1076.

Akashi H. 1996. Molecular evolution between *Drosophila melanogaster* and *D. simulans*: Reduced codon bias, faster rates of amino acid substitution, and larger proteins in *D. melanogaster*. *Genetics* **144**: 1297–1307.

Akashi H, Schaeffer SW. 1997. Natural selection and the frequency distributions of “silent” DNA polymorphism in *Drosophila*. *Genetics* **146**: 295–307.

Andolfatto P. 2001. Contrasting patterns of X-linked and autosomal nucleotide variation in *Drosophila melanogaster* and *Drosophila simulans*. *Mol Biol Evol* **18**: 279–290.

Andolfatto P. 2005. Adaptive evolution of non-coding DNA in *Drosophila*. *Nature* **437**: 1149–1152.

Andolfatto P, Davison D, Erezylmaz D, Hu TT, Mast J, Sunayama-Morita T, Stern DL. 2011a. Multiplexed shotgun genotyping for rapid and efficient genetic mapping. *Genome Res* **21**: 610–617.

Andolfatto P, Wong KM, Bachtrog D. 2011b. Effective population size and the efficacy of selection on the X chromosomes of two closely related *Drosophila* species. *Genome Biol Evol* **3**: 114–128.

Aquadro CF, Lado KM, Noon WA. 1988. The rosy region of *Drosophila melanogaster* and *Drosophila simulans*. I. Contrasting levels of naturally occurring DNA restriction map variation and divergence. *Genetics* **119**: 875–888.

Ballard JW. 2000. Comparative genomics of mitochondrial DNA in members of the *Drosophila melanogaster* subgroup. *J Mol Evol* **51**: 48–63.

Begun DJ. 2001. The frequency distribution of nucleotide variation in *Drosophila simulans*. *Mol Biol Evol* **18**: 1343–1352.

Begun DJ, Holloway AK, Stevens K, Hillier LW, Poh YP, Hahn MW, Nista PM, Jones CD, Kern AD, Dewey CN, et al. 2007. Population genomics: Whole-genome analysis of polymorphism and divergence in *Drosophila simulans*. *PLoS Biol* **5**: e310. doi: 10.1371/journal.pbio.0050310.

Bradley RK, Roberts A, Smoot M, Juvekar S, Do J, Dewey C, Holmes I, Pachter L. 2009. Fast statistical alignment. *PLoS Comput Biol* **5**: e1000392. doi: 10.1371/journal.pcbi.1000392.

Callahan B, Neher RA, Bachtrog D, Andolfatto P, Shraiman BI. 2011. Correlated evolution of nearby residues in *Drosophilid* proteins. *PLoS Genet* **7**: e1001315. doi: 10.1371/journal.pgen.1001315.

Cao J, Schneeberger K, Ossowski S, Günther T, Bender S, Fitz J, Koenig D, Lanz C, Stegle O, Lippert C, et al. 2011. Whole-genome sequencing of multiple *Arabidopsis thaliana* populations. *Nat Genet* **43**: 956–963.

Charlesworth B. 2009. Fundamental concepts in genetics: Effective population size and patterns of molecular evolution and variation. *Nat Rev Genet* **10**: 195–205.

Charlesworth B. 2010. Molecular population genomics: A short history. *Genet Res* **92**: 397–411.

Charlesworth B, Coyne J, Barton NH. 1987. The relative rates of evolution of sex chromosomes and autosomes. *Am Nat* **130**: 113–146.

Charlesworth B, Morgan MT, Charlesworth D. 1993. The effect of deleterious mutations on neutral molecular variation. *Genetics* **134**: 1289–1303.

Charlesworth B, Betancourt AJ, Kaiser VB, Gordo I. 2009. Genetic recombination and molecular evolution. *Cold Spring Harb Symp Quant Biol* **74**: 177–186.

*Drosophila* 12 Genomes Consortium, Clark AG, Eisen MB, Smith DR, Bergman CM, Oliver B, Markow TA, Kaufman TC, Kellis M, Gelbart W, et al. 2007. Evolution of genes and genomes on the *Drosophila* phylogeny. *Nature* **450**: 203–218.

Edgar RC. 2004. MUSCLE: A multiple sequence alignment method with reduced time and space complexity. *BMC Bioinformatics* **5**: 113. doi: 10.1186/1471-2105-5-113.

Eyre-Walker A, Keightley PD. 2007. The distribution of fitness effects of new mutations. *Nat Rev Genet* **8**: 610–618.

Fay JC, Wyckoff GJ, Wu CI. 2002. Testing the neutral theory of molecular evolution with genomic data from *Drosophila*. *Nature* **415**: 1024–1026.

Gnad F, Parsch J. 2006. Sebida: A database for the functional and evolutionary analysis of genes with sex-biased expression. *Bioinformatics* **22**: 2577–2579.

Hadrill PR, Bachtrog D, Andolfatto P. 2008. Positive and negative selection on noncoding DNA in *Drosophila simulans*. *Mol Biol Evol* **25**: 1825–1834.

Halligan DL, Keightley PD. 2006. Ubiquitous selective constraints in the *Drosophila* genome revealed by a genome-wide interspecies comparison. *Genome Res* **16**: 875–884.

Jukes T, Cantor C. 1969. Evolution of protein molecules. In *Mammalian protein metabolism*. III (ed. HN Munro), pp. 21–132. Academic Press, New York.

Kelley DR, Schatz MC, Salzberg SL. 2010. Quake: Quality-aware detection and correction of sequencing errors. *Genome Biol* **11**: R116. doi: 10.1186/gb-2010-11-11-r116.

Kent WJ. 2002. BLAT—the BLAST-like alignment tool. *Genome Res* **12**: 656–664.

Kimura M. 1983. *The neutral theory of molecular evolution*. Cambridge University Press, Cambridge, UK.

Kurtz S, Phillippy A, Delcher AL, Smoot M, Shumway M, Antonescu C, Salzberg SL. 2004. Versatile and open software for comparing large genomes. *Genome Biol* **5**: R12. doi: 10.1186/gb-2004-5-2-r12.

Li H, Handsaker B, Wysoker A, Fennell T, Ruan J, Homer N, Marth G, Abecasis G, Durbin R, Subgroup GPPD. 2009. The Sequence Alignment/Map format and SAMtools. *Bioinformatics* **25**: 2078–2079.

Mackay TFC, Richards S, Stone EA, Barbadilla A, Ayroles JF, Zhu D, Casillas S, Han Y, Magwire MM, Cridland JM, et al. 2012. The *Drosophila melanogaster* Genetic Reference Panel. *Nature* **482**: 173–178.

Mank JE, Vicoso B, Berlin S, Charlesworth B. 2010. Effective population size and the Faster-X effect: Empirical results and their interpretation. *Evolution* **64**: 663–674.

- McVean GA, Vieira J. 2001. Inferring parameters of mutation, selection and demography from patterns of synonymous site evolution in *Drosophila*. *Genetics* **157**: 245–257.
- Moriyama EN, Powell JR. 1996. Intraspecific nuclear DNA variation in *Drosophila*. *Mol Biol Evol* **13**: 261–277.
- Nielsen R, Bauer DuMont VL, Hubisz MJ, Aquadro CF. 2007. Maximum likelihood estimation of ancestral codon usage bias parameters in *Drosophila*. *Mol Biol Evol* **24**: 228–235.
- Ning Z, Cox AJ, Mullikin JC. 2001. SSAHA: A fast search method for large DNA databases. *Genome Res* **11**: 1725–1729.
- Ohta T. 1973. Slightly deleterious mutant substitutions in evolution. *Nature* **246**: 96–98.
- Ohta T. 1993. Amino acid substitution at the *Adh* locus of *Drosophila* is facilitated by small population size. *Proc Natl Acad Sci* **90**: 4548–4551.
- Parsch J, Novozhilov S, Saminadin-Peter SS, Wong KM, Andolfatto P. 2010. On the utility of short intron sequences as a reference for the detection of positive and negative selection in *Drosophila*. *Mol Biol Evol* **27**: 1226–1234.
- Petrov DA, Hartl DL. 1999. Patterns of nucleotide substitution in *Drosophila* and mammalian genomes. *Proc Natl Acad Sci* **96**: 1475–1479.
- Smith NGC, Eyre-Walker A. 2002. Adaptive protein evolution in *Drosophila*. *Nature* **415**: 1022–1024.
- Sturgill D, Zhang Y, Parisi M, Oliver B. 2007. Demasculinization of X chromosomes in the *Drosophila* genus. *Nature* **450**: 238–241.
- Treangen TJ, Salzberg SL. 2012. Repetitive DNA and next-generation sequencing: Computational challenges and solutions. *Nat Rev Genet* **13**: 36–46.
- Vicario S, Moriyama EN, Powell JR. 2007. Codon usage in twelve species of *Drosophila*. *BMC Evol Biol* **7**: 226. doi: 10.1186/1471-2148-7-226.
- Vicoso B, Charlesworth B. 2006. Evolution on the X chromosome: Unusual patterns and processes. *Nat Rev Genet* **7**: 645–653.
- Wilson DJ, Hernandez RD, Andolfatto P, Przeworski M. 2011. A population genetics–phylogenetics approach to inferring natural selection in coding sequences. *PLoS Genet* **7**: e1002395. doi: 10.1371/journal.pgen.1002395.
- Wright S, Andolfatto P. 2008. The impact of natural selection on the genome: Emerging patterns in *Drosophila* and *Arabidopsis*. *Annu Rev Ecol Evol Syst* **39**: 193–213.
- Yang Z. 2007. PAML 4: Phylogenetic analysis by maximum likelihood. *Mol Biol Evol* **24**: 1586–1591.
- Zerbino DR, Birney E. 2008. Velvet: Algorithms for de novo short read assembly using de Bruijn graphs. *Genome Res* **18**: 821–829.
- Zhang Y, Sturgill D, Parisi M, Kumar S, Oliver B. 2007. Constraint and turnover in sex-biased gene expression in the genus *Drosophila*. *Nature* **450**: 233–237.

Received April 12, 2012; accepted in revised form August 29, 2012.